NeuroImage: Clinical 12 (2016) 234–240

Contents lists available at ScienceDirect

NeuroImage: Clinical

journal homepage: www.elsevier.com/locate/ynicl

Discriminating among degenerative parkinsonisms using advanced ^{123}I-ioflupane SPECT analyses

Simon Badoud[a,b,c], Dimitri Van De Ville[d,e], Nicolas Nicastro[a], Valentina Garibotto[c,f], Pierre R. Burkhard[a,c], Sven Haller[c,g,h,i,*]

[a] Neurology Division, Department of Clinical Neurosciences (NEUCLI), Geneva University Hospitals, Switzerland
[b] Neurophysiology Unit, Department of Medicine, University of Fribourg (CH), Switzerland
[c] Faculty of Medicine, University of Geneva, Switzerland
[d] Department of Imaging and Medical Informatics, University Hospitals of Geneva, Faculty of Medicine, University of Geneva, Switzerland
[e] Institute of Bioengineering, Ecole Polytechnique Fédérale de Lausanne, Switzerland
[f] Nuclear Medicine and Molecular Imaging Division, Department of Imaging and Medical Informatics, University Hospitals of Geneva, Switzerland
[g] Affidea Centre de Diagnostic Radiologique de Carouge CDRC, Geneva, Switzerland
[h] Department of Surgical Sciences, Radiology, Uppsala University, Uppsala, Sweden
[i] Department of Neuroradiology, University Hospital Freiburg, Germany

ARTICLE INFO

Article history:
Received 9 May 2016
Received in revised form 23 June 2016
Accepted 4 July 2016
Available online 05 July 2016

Keywords:
Parkinson's disease
Atypical parkinsonism
Single photon emission computed tomography (SPECT)
Multi vector pattern analysis (MVPA)

ABSTRACT

^{123}I-ioflupane single photon emission computed tomography (SPECT) is a sensitive and well established imaging tool in Parkinson's disease (PD) and atypical parkinsonian syndromes (APS), yet a discrimination between PD and APS has been considered inconsistent at least based on visual inspection or simple region of interest analyses. We here reappraise this issue by applying advanced image analysis techniques to separate PD from the various APS.

This study included 392 consecutive patients with degenerative parkinsonism undergoing ^{123}I-ioflupane SPECT at our institution over the last decade: 306 PD, 24 multiple system atrophy (MSA), 32 progressive supranuclear palsy (PSP) and 30 corticobasal degeneration (CBD) patients. Data analysis included voxel-wise univariate statistical parametric mapping and multivariate pattern recognition using linear discriminant classifiers.

MSA and PSP showed less ioflupane uptake in the head of caudate nucleus relative to PD and CBD, yet there was no difference between MSA and PSP. CBD had higher uptake in both putamen relative to PD, MSA and PSP. Classification was significant for PD versus APS (AUC 0.69, $p < 0.05$) and between APS subtypes (MSA vs CBD AUC 0.80, $p < 0.05$; MSA vs PSP AUC 0.69 $p < 0.05$; CBD vs PSP AUC 0.69 $p < 0.05$).

Both striatal and extra-striatal regions contain classification information, yet the combination of both regions does not significantly improve classification accuracy.

PD, MSA, PSP and CBD have distinct patterns of dopaminergic depletion on ^{123}I-ioflupane SPECT. The high specificity of 84–90% for PD versus APS indicates that the classifier is particularly useful for confirming APS cases.

1. Introduction

With a prevalence ranging from 1 to 2% in the population above 65 years of age, Parkinson's disease (PD) is the most common neurodegenerative movement disorder. Other less common forms of degenerative parkinsonism, collectively referred to as atypical parkinsonian syndromes (APS), include multiple system atrophy (MSA), progressive supranuclear palsy (PSP) and corticobasal degeneration (CBD). Whereas a clinical diagnosis of PD can be established with accuracy superior to 90% when assessed by an experienced movement disorders specialist, this is not the case for APS where diagnostic accuracy varies between 50 and 80% at the very best. This diagnosis issue is even more problematic at early stages when all suggestive features are not present (Hughes et al., 2002). Dissecting apart degenerative parkinsonisms is however important with respect to both treatment and prognosis. While PD patients typically respond well to dopamine replacement therapy, have a slower progression and a good prognosis at 10 years, APS typically respond less or not at all to dopaminergic medications, have a more rapid disease course and a much worse outcome.

Neuroimaging may complement clinical assessment and ^{123}I-ioflupane single photon emission computed tomography (SPECT) has recently become a reliable clinical imaging tool to assess the integrity of the nigrostriatal dopaminergic system (Brücke et al., 1997;

Abbreviations: APS, atypical parkinsonian syndromes; CBD, corticobasal degeneration; MSA, multiple system atrophy; MVPA, Multi Voxel Pattern Analysis; PD, Parkinson's disease; PSP, progressive supranuclear palsy; ROI, region of interest; SPECT, single photon emission computed tomography; SVM, support vector machines.

* Corresponding author at: Affidea Centre de Diagnostic Radiologique de Carouge CDRC, Geneva, Switzerland.
E-mail address: sven.haller@gmail.com (S. Haller).

http://dx.doi.org/10.1016/j.nicl.2016.07.004

Cummings et al., 2011). This technique has a high sensitivity to detect PD versus controls even at an early stage, yet the pattern of alterations of the dopaminergic system is quite similar between PD and APS (Brücke et al., 1997; Kägi et al., 2010; Sixel-Döring et al., 2011). Consequently, simple visual or region of interest (ROI)-based analyses, as routinely performed in most centers, do not seem to allow a robust distinction between PD and APS (Brooks, 2012; Kägi et al., 2010; Klaffke et al., 2006; Marek et al., 2000; Pirker et al., 2000a), so that ^{123}I-ioflupane SPECT is currently not recommended for the differential diagnosis of degenerative parkinsonism.

The current investigation intends to reappraise this diagnostic issue based on the assumption that systematic but subtle differences in ^{123}I-ioflupane SPECT between PD and APS can be consistently detected using advanced data analysis techniques. Previous investigations applying support vector machines (SVM), a type of Multi Voxel Pattern Analysis (MVPA), successfully discriminated PD from APS patients based on MRI diffusion tensor imaging (DTI) (Haller et al., 2012), MRI susceptibility weighted imaging (SWI) (Haller et al., 2013) and gait analysis (Tahir and Manap, 2012). This SVM classification technique was also applied to ^{123}I-ioflupane SPECT data to discriminate 95 PD versus 94 controls (Segovia et al., 2012) and to discriminate 56 PD versus 34 non-PD (essential tremor and drug-induced parkinsonism) patients (Palumbo et al., 2014). A comparison between PD and APS was not performed as yet.

The present study includes a large cohort of 392 consecutive patients with a clinical diagnosis of PD, MSA, PSP and CBD scanned on the same tomograph, in the same center over a period of 10 years. We performed univariate statistical parametric mapping and multivariate pattern recognition classification analyses to test the hypothesis that PD and APS have distinct patterns of dopaminergic depletion on ^{123}I-ioflupane SPECT, which may enable a clinically useful discrimination between groups.

2. Materials and methods

2.1. Participants

The present retrospective study was approved by the local ethics committee and includes 970 consecutive patients undergoing ^{123}I-ioflupane SPECT scanning in our institution between October 2003 and September 2013. 392 participants met our inclusion criteria: 1) ^{123}I-ioflupane SPECT of high quality, 2) extensive neurological assessment and 3) clinical follow-up over many years for most patients, and 4) no significant morphological findings on structural images based on magnetic resonance imaging (MRI) unrelated to neurodegeneration. UK Parkinson's disease society brain bank criteria were used for the diagnosis of PD. They include the presence of bradykinesia associated with one of the following criteria: 4–6 Hz rest tremor, rigidity or postural instability. Other supportive criteria considered as essential were a very good and sustained response to levodopa, development of typical levodopa-induced dyskinesia, a unilateral onset and a slowly progressive course. This assessment was achieved by an experienced movement disorders specialist. Regarding APS diagnoses, we strictly applied well-established, validated and recent criteria, including the second consensus statement for the diagnosis of MSA (Gilman et al., 2008), the National Institute of Neurological Disorders Society (NINDS) clinical research criteria for PSP (Litvan et al., 1996) and the criteria for the diagnosis of CBD proposed by (Armstrong et al., 2013). Cases who did not fulfill those sets of criteria were excluded. Thanks to the usually long follow-up period for most cases, 12 out of the 392 included patients (3.1%) had their diagnosis changed over time (PD for MSA in 4, PD for PSP in 2, MSA for PD in 2, CBD for PD in 2, PSP for CBD in 1 and CBD for PSP in 1). In these cases, only the most recent diagnosis was considered for classification.

It is important to note that the ^{123}I-ioflupane SPECT was not used to confirm a specific diagnosis but to exclude non-degenerative parkinsonisms. Similarly, MRI was performed to exclude secondary forms of parkinsonism, such as vascular parkinsonism or normal pressure hydrocephalus, but not as a supportive diagnostic biomarker for PD or APS.

The final sample included 306 PD patients (54% male, age 69.4 ± 11 years, disease duration 2.4 ± 0.9 years at the time of scan) 24 MSA (54% males, age 64.6 ± 10.0 years, disease duration 3.2 ± 3.1 years), 32 PSP (66% males, age 72.9 ± 8.3 years, disease duration 1.9 ± 1.2 years) and 30 CBD (53% males, age 73.9 ± 7.1 years, disease duration 2.4 ± 1.8 years). 301 of the 306 PD patients were reported in a previous investigation, which describes the spatio-temporal pattern of dopaminergic depletion in PD (Badoud et al., 2016), and re-used as a reference group in the current investigation. In contrast, the current investigation aims to classify APS, which were not included in the previous investigation. According to the ANOVA multiple comparison test, there was no significant difference between groups concerning the sex ratio. The ANOVA test revealed significant differences between groups in terms of age ($p = 0.019$) and disease duration ($p = 0.007$) (see Table 1).

2.2. SPECT image acquisition

Sodium perchlorate or Lugol solution were preventively administered to the patients in order to block thyroid uptake. Patients were scanned on a triple-head gamma-camera (Toshiba Medical Systems, Tokyo, Japan) with fan-beam, low-energy, high-resolution collimators, 4 h after intravenous injection of about 185 MBq of ^{123}I-ioflupane SPECT, following a standard protocol described in details elsewhere (Garibotto et al., 2013). Images were corrected for scatter using a triple-energy window method and for a uniform attenuation correction.

2.3. MR image acquisition

Variable MRI protocols were performed according to clinical routine procedures that evolved over the 10-year study period. However a minimum of a T2, fluid attenuation inversion recovery (FLAIR) and diffusion weighted imaging (DWI) or diffusion tensor imaging (DTI) were available in all participants to exclude structural brain lesions. In addition, the integrity of white matter was analyzed using the Fazekas score (Fazekas et al., 1987).

103 patients had a high-resolution Magnetization Prepared Rapid Gradient Echo (MPRAGE) 3DT1brain scan performed on 3.0 Tesla MR system (Magnetom Trio, Siemens, Erlangen Germany) as part of our clinical routine protocol (256 × 256 matrix, 176 sections, $1 \times 1 \times 1$ mm^3, TE = 2.3 ms, TR = 2300 ms). This subsample was used to build a ^{123}I-ioflupane SPECT template in Montreal Neurological Institute (MNI) standard space as described earlier (Badoud et al., 2016; García-Gómez et al., 2013).

2.4. Statistical analyses

FSL (FMRIB Software Library version 5.0 http://fsl.fmrib.ox.ac.uk/fsl/fslwiki), Graphpad Prim (version 6.0, www.graphpad.com), and Matlab (version R2014a) were used for statistical analyses and classification.

Table 1
Demographic and clinical characteristics.

	PD	APS			Stat.
		MSA	PSP	CBD	
Sex (m/f)	164/142	13/11	21/11	16/14	n.s
Age (year)	69.4 ± 11	64.6 ± 10.0	72.9 ± 8.3	73.9 ± 7.1	**
Disease duration (year)	2.4 ± 0.9	3.2 ± 3.1	1.9 ± 1.2	2.4 ± 1.8	*

This table summarized the essential demographic data of the patient groups.
* $p < 0.05$.
** $p < 0.01$.

2.5. Image post-processing

We used a ^{123}I-ioflupane SPECT template in Montreal Neurological Institute (MNI) standard space as described earlier (Badoud et al., 2016; García-Gómez et al., 2013) in an automatic and operator-independent workflow. Due to the asymmetrical degeneration of the nigrostriatal pathways in PD and APS, we decided to flip all patients presenting predominant clinical symptoms on the left side of the body in order to obtain a more homogeneous sample with dominant symptomatology always at the same hemisphere. Equivalent to previous investigations and existing software packages, intensity was normalized with respect to the occipital lobe, both for striatal and extra-striatal signals.

2.6. Voxel-wise statistical analysis

The voxel-wise statistical analysis was done using the randomize function of FSL by permutation testing ($n = 5000$) and Threshold-Free Cluster enhancement (TFCE) error multiple comparisons correction at $p < 0.05$ considered as significant (Smith and Nichols, 2009). Age and gender were used as non-explanatory co-regressors to eliminate potential bias linked to age or gender. Analyses described in this paragraph were performed inside a striatal mask including the putamen and the caudate nuclei. The mask was created using the Harvard subcortical atlas included in FSL.

2.7. Classification analysis

We used a combination of simple linear classifiers (i.e., linear discriminant analysis) for which each is given a random subset of the feature space. Putting together such weak learners in an ensemble leads to flexible yet robust models (Rokach, 2010). We used the ensemble classifier as implemented in the Matlab Statistics Toolbox (R2014b). The total number of learners was set to 1500 and the prior probabilities of the patient labels were assumed uniformly distributed to compensate for the unequal number of subjects in each category. To reduce the dimensionality and exploit spatial correlation - the total number of voxels was 4916 in the striatum mask and 253,454 in the whole-brain mask (without striatum, occipital lobe included) - we applied the singular value decomposition to the data of each patient group (within the cross-validation fold) and retained 20 and 30 components that corresponded to 94% and 99% of the explained variance for the striatum and whole-brain mask, respectively. All training subjects were then projected onto the principal components of each group, which led to a total number of features of 80 and 120 for classification based on the striatum and whole-brain mask, respectively. The classification accuracy was evaluated using leave-one-subject-out cross-validation with strict separation of training and test data. Based on this classifier, we performed ROC analysis for the classification of PD versus APS and between the APS classes. The significance of the AUC measures was obtained by establishing its null distribution under random permutations of the patient labels.

3. Results

3.1. Voxel-wise group-level statistical analysis

Group comparisons were performed in two steps. The first one consisted in comparing the differences of dopaminergic uptakes between PD and APS, while the second one investigated the differences between APS.

3.2. PD versus APS

The voxel-wise analysis revealed a significantly lower ^{123}I-ioflupane uptake in all APS versus PD in the head of caudate nucleus ($p < 0.002$). The Cohen's d standardized measure of effect size (Friston, 2012) for this cluster is 0.55, which indicates a medium effect. The inverse comparison showed a cluster located on the ipsilateral putamen with increased ^{123}I-ioflupane uptake in APS compared to PD ($p < 0.05$); the Cohen's $d = -0.43$ indicates a small-to-medium effect size.

Concerning the different types of APS, MSA and PSP exhibited a significantly lower ^{123}I-ioflupane uptake in the head of the caudate nucleus ($p < 0.002$) compared to PD. The effect sizes are $d = 0.31$ and $d = 0.86$, respectively. The inverse comparison led to no significant results.

CBD versus PD revealed increased ^{123}I-ioflupane uptake in the putamen bilaterally. The effect size $d = 0.99$ is large. The inverse comparison revealed no significant differences (Fig. 1).

3.3. APS versus APS

The comparison within the group of APS, i.e. MSA versus PSP versus CBD revealed significantly lower ^{123}I-ioflupane uptake in MSA and PSP compared to CDB in both putamen and the posterior part of the head of the caudate nucleus, with the head of the caudate nucleus being more affected in PSP (Fig. 2). The inverse comparison did not yield any supra-threshold clusters.

The comparison between MSA versus PSP revealed no supra-threshold clusters.

3.4. Classification analysis

Although sensitivity in the classification PD vs APS was low, the high specificity (84% striatum only; 90% whole brain) showed that APS could be identified well. All AUC measures (68% striatum only; 69% whole brain) are significant ($p < 0.05$).

While voxels in the striatum mask were informative for the classification, the use of the whole-brain mask without the striatum was informative as well. The whole-brain mask with striatum did not improve accuracies, which indicates that information was redundant inside and outside the striatum mask, but not complementary.

The classification was also significant for all APS subtypes (MSA vs CBD AUC0.80, $p < 0.05$; MSA vs PSP AUC 0.69 $p < 0.05$; CBD vs PSP AUC 0.69 $p > 0.05$). The results for discriminating PD versus APS and between APS are illustrated in Table 2. The corresponding ROC curves are illustrated in Fig. 3.

4. Discussion

In this study, we were able to demonstrate distinct patterns of dopaminergic depletion for PD, MSA, PSP and CBD using ^{123}I-ioflupane SPECT in a sample of 392 consecutive patients. Multivariate pattern recognition of ^{123}I-ioflupane SPECT discriminated PD, PSP and CBD and MSA. The classification accuracies should be interpreted with respect to the clinical diagnostic accuracy in particular at early stages of the disease (Hughes et al., 2002; Italian Neurological Society, 2003) and in light of the classic view that standard analyses of ^{123}I-ioflupane SPECT do not discriminate PD and degenerative APS (Brooks, 2012; Kägi et al., 2010; Marek et al., 2000; Pirker et al., 2000a).

4.1. PD versus APS

Our results showed that the atypical forms of parkinsonism, notably MSA, PSP and CBD, seem to affect the ^{123}I-ioflupane striatal uptake following a topographically distinct pattern compared to PD. MSA and PSP have a significantly lower ^{123}I-ioflupane uptake in the caudate nucleus, whereas, conversely, CBD demonstrated an increased ^{123}I-ioflupane uptake indicating less pronounced dopaminergic depletion in the putamen as compared to PD.

Due to the fact that the various types of APS have distinct patterns of nigrostriatal degeneration, the direct comparison between PD and all APS taken together is thus confounded by the differences in the spatial

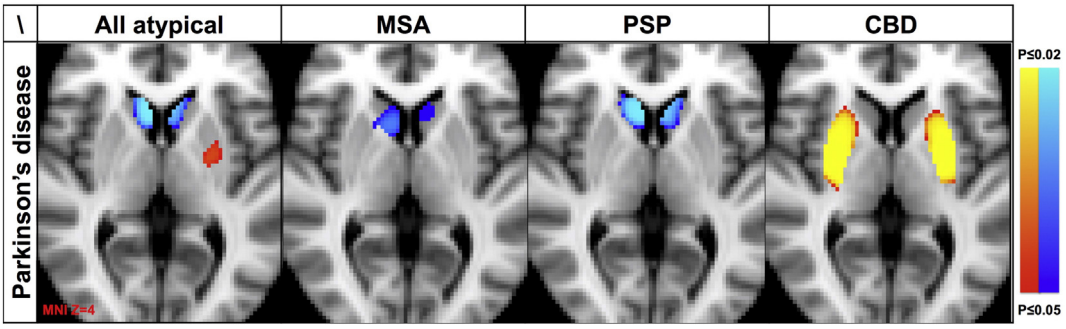

Fig. 1. Illustrates the comparison between all APS confounded, only MSA, only PSP and only CBD versus PD. APS in general and MSA and PSP in particular, showed a decreased ^{123}I-ioflupane uptake in the head of caudate nucleus bilaterally yet an increased ^{123}I-ioflupane uptake in ipsilateral putamen. CBD versus PD had an increased ^{123}I-ioflupane uptake in the head of the caudate nucleus bilaterally. ^{123}I-ioflupane uptake maps superimposed on axial T1 weighted MRI in Montreal Neurological Institute (MNI) standard space with the clinically dominant symptomatic side on the right hemisphere. Threshold-Free Cluster enhancement (TFCE) error multiple comparisons correction at $p < 0.05$.

pattern of dopaminergic depletion in MSA, PSP and CBD and consequently potentially confounded by the group size composition.

4.2. Specific patterns of dopaminergic depletion in APS

The MSA group had significantly more pronounced dopaminergic depletion in the head of caudate nucleus bilaterally as compared to PD. This result is consistent with a previous [^{123}I]β-CIT SPECT study in 8 MSA versus 11 PD patients, demonstrating a significant decrease of SPECT signal in the head of the caudate nucleus and the anterior part of the putamen in the MSA group (Nocker et al., 2012). Moreover, and in line with the current results, several investigations previously reported a decreased ^{123}I-ioflupane uptake in MSA as compared to PD (Pirker et al., 2000a; Varrone et al., 2001).

However, at variance with our study, the results presented by Pirker et al. were obtained by calculating values in manually drawn ROI that could introduce important variability in the data (Pirker et al., 2000a). Similarly, Varrone and colleagues did not perform spatial normalization before setting their ROI template. This method is also at risk of introducing a measurement bias (Varrone et al., 2001). Finally, Scherfler and colleagues chose to conduct voxel-wise analysis using statistical parametric mapping software (SPM) following the same line as our protocol (Scherfler et al., 2005). Nevertheless, they achieved spatial normalization through an indirect method consisting of transferring the [^{123}I]β-CIT SPECT images to a ^{18}F-DOPA PET template whereas we decided to create a study specific functional template for the exact modality needed (^{123}I-ioflupane SPECT).

The asymmetrical pattern of PD versus MSA, showing a more significant decrease on the contralateral side, can be related to the fact that the contra/ipsilateral signal asymmetry is likely to be more pronounced in PD than in MSA (Varrone et al., 2001).

Concerning PSP, the dopaminergic depletion is also more pronounced in the head of the caudate nucleus as compared to PD. This pattern is similar to the MSA pattern discussed above.

Previous investigations demonstrated that PSP is characterized by a more uniform reduction of the striatal dopaminergic uptake both in the caudate nucleus and the putamen and by a low left/right asymmetry (Antonini et al., 2003; Brooks, 2010). Globally, the dopaminergic nigrostriatal pathway seems to be more severely affected in PSP than in PD (Brooks et al., 1990). In agreement with our results, a previous [^{123}I]β-CIT SPECT study in 14 PSP patients and 17 PD patients demonstrates a significantly lower signal in the caudate nuclei in the PSP group (Seppi et al., 2006).

With respect to CBD, there is increased ^{123}I-ioflupane uptake representing less dopaminergic depletion in bilateral putamen as compared to PD. These results indicate that CBD affects the dopaminergic system less severely in the putamen and are consistent with the observation that the dopaminergic system is less severely affected in CBD as

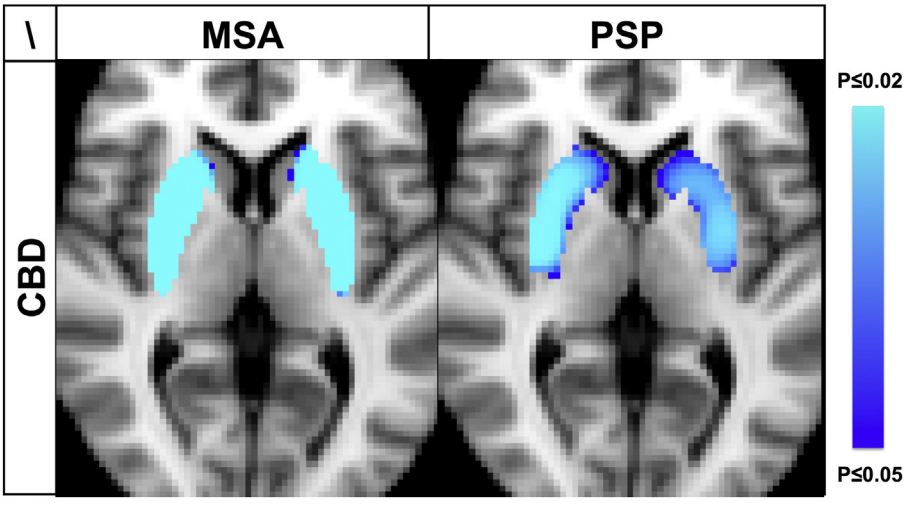

Fig. 2. MSA and PSP versus CBD had decreased ^{123}I-ioflupane uptake in putamen and head of caudate nucleus bilaterally. The inverse comparison between CBD versus MSA or PSP as well as the comparison between MSA versus PSP revealed no supra-threshold clusters. Illustration equivalent to Fig. 1.

Table 2
Classification results in terms of sensitivity and specificity (first line) and area-under-curve (AUC) of the ROC analysis (second line). All the AUC measures are significant ($p < 0.05$).

	PD vs APS	APS		
		MSA vs CBD	MSA vs PSP	CBD vs PSP
Striatum only	45%/84%	75%/86%	50%/71%	69%/65%
	0.68, $p < 0.05$	0.79, $p < 0.05$	0.67, $p < 0.05$	0.63, $p < 0.05$
Extra-striatum	26%/86%	55%/84%	50%/75%	67%/71%
	0.68, $p < 0.05$	0.76, $p < 0.05$	0.68, $p < 0.05$	0.69, $p < 0.05$
Whole-brain	28%/90%	78%/95%	58%/71%	67%/65%
	0.69, $p < 0.05$	0.80, $p < 0.05$	0.69, $p < 0.05$	0.68, $p < 0.05$

compared to PD (Pirker et al., 2000a). In rare instances of neuropathologically proven CBD cases, ^{123}I-ioflupane uptake has even been found normal (Kaasinen et al., 2013).

4.3. MSA versus PSP versus CBD

MSA and PSP exhibit significantly stronger dopaminergic depletion in the head of caudate nucleus and putamen as compared to CBD. These results are not in line with the study published by Pirker and colleagues suggesting no significant difference between CBD, PSP and MSA in terms of dopaminergic denervation (Pirker et al., 2000b). However, the authors conducted an analysis comparing the average striatal activities and included only four CBD patients.

4.4. Classification

The accuracy of PD versus APS is about 68% and the high specificity (84–90%) indicates that the classifier is particularly useful for confirming APS cases. Discriminating between APS cases has highest accuracies for MSA versus CBD, and slightly less for MSA versus PSP and CBD versus PSP.

Two previous investigations by Palumbo et al. and by Segovia et al. assessed classification performance of PD versus controls (Palumbo et al., 2014; Segovia et al., 2012). Note that the classification accuracies of 73.9% and 94.7%, respectively, exceed the classification accuracy of the current investigation due to the fact that the discrimination of a disease condition associated with a clear dopaminergic depletion versus a healthy control group is much easier than the classification of several disease conditions which significantly affect the dopaminergic system. Even if some subtle differences in ^{123}I-Ioflupane uptake between PD and APS were previously reported, there is a general agreement that these differences are subtle and consequently the visual inspection of ^{123}I-ioflupane uptake maps does not allow for an accurate diagnosis (Brooks, 2012; Kägi et al., 2010; Marek et al., 2000; Pirker et al., 2000a). The presented operator-independent classification analysis of the complex pattern of dopaminergic depletion, which provided

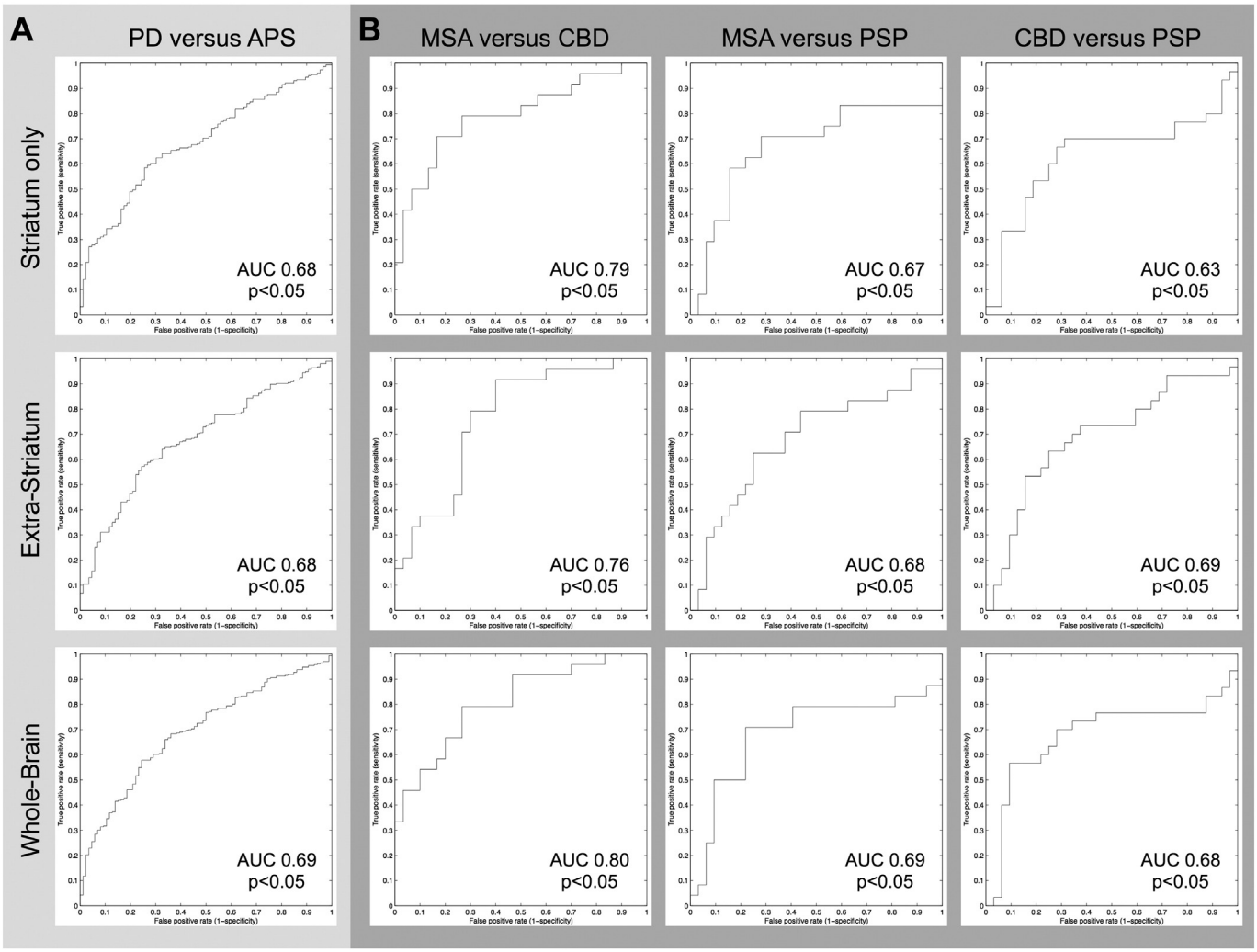

Fig. 3. Receiver-operating-characteristics (ROC) curves that show the specificity/sensitivity trade-off of the classifiers for PD versus all APS (A) and in-between APS subtypes MSA, CBD and PSP (B).

above-chance classification accuracy, is therefore an added value for the clinical diagnosis of individual patients.

4.5. Striatal versus extra-striatal signal

The ^{123}I-ioflupane uptake is most pronounced in the nigrostriatal system (Booij et al., 1997a, 1997b), and, consequently, most previous investigations have focused on this brain region. Based on the assumption that PD and APS might also affect the ^{123}I-Ioflupane uptake outside the striatum, we performed the classification analysis three times, once only within the striatum, once in the remaining brain outside the striatum, and once using the entire brain. As expected, the striatum was most informative for the classification. Nevertheless, above-chance classification was possible even when considering only the regions outside the striatum. This indicates that dopaminergic impairment of extra-striatal brain regions in PD and APS can be evaluated by advanced analysis techniques of molecular imaging. Yet, some studies have put in light an affinity of ^{123}I-Ioflupane for noradrenergic and serotoninergic receptors, especially within extrastriatal areas (Koch et al., 2014). Thus, non-dopaminergic uptake has to be taken into account for the interpretation of our results. Indeed, PD has been shown to be also associated with non-dopaminergic modifications (H. Braak and E. Braak, 2000). The whole-brain analysis did not improve accuracies, which might indicate that information was redundant inside and outside the striatum, but not complementary. While previous studies suggested that the striatum was the only region to provide relevant information regarding the state of the nigrostriatal pathway (Gaig et al., 2006; Seibyl et al., 2013), our results indicate that extra-striatal regions also convey relevant information. For example, one recent investigation indicates that extra-striatal ^{123}I-ioflupane modification can be observed in the context of addiction (Leroy et al., 2012). In PD, extra-striatal dopaminergic impairment has been demonstrated, notably in ventral midbrain (Joutsa et al., 2015). An interesting avenue for future research is to investigate to what extent the discriminative information relies on textural features.

4.6. Strengths and limitations

The large cohort used for this study (392 patients) represents its major asset. Additionally, all patients were scanned consecutively on the same machine using the same protocol of acquisition. In order to avoid operator-related variability, all post-processing procedures were conducted in an operator-independent manner including the creation of a study specific template. Sex and age data were used as non-explanatory co-regressors in order to compensate for their well-known impact on the nigrostriatal pathway (Nicastro et al., 2016).

The retrospective nature of this study is an important limitation, yet the clinical follow-up, typically of several years for most patients, allowed some diagnostic reallocation, which may also be seen as an advantage for the purpose of this diagnosis-oriented study. Moreover, an impact of anti-parkinsonian medications on the images cannot be totally excluded even if several studies have not shown significant consequences regarding ^{123}I-FP CIT SPECT acquisition (Ahlskog et al., 1999). Finally, neuropathological data were not available for the vast majority of patients, so that diagnosis of PD and APS is based on well-established clinical diagnostic criteria.

Author contributions

SB: data collection, data analysis, manuscript preparation.
DVDV: data analysis, manuscript preparation.
NN: data collection, manuscript preparation.
VG: data collection, manuscript preparation.
PB: clinical assessment, study supervision, manuscript preparation.
SH: study design, study supervision, data analysis, manuscript preparation.

Disclosure

No conflicts of interest.

References

Ahlskog, J.E., Uitti, R.J., O'Connor, M.K., Maraganore, D.M., Matsumoto, J.Y., Stark, K.F., Turk, M.F., Burnett, O.L., 1999. The effect of dopamine agonist therapy on dopamine transporter imaging in Parkinson's disease. Mov. Disord. 14, 940–946. http://dx.doi.org/10.1002/1531-8257(199911)14:6<940::AID-MDS1005>3.0.CO;2-Y.

Antonini, A., Benti, R., De Notaris, R., Tesei, S., Zecchinelli, A., Sacilotto, G., Meucci, N., Canesi, M., Mariani, C., Pezzoli, G., Gerundini, P., 2003. I-123-Ioflupane/SPECT binding to striatal dopamine transporter (DAT) uptake in patients with Parkinson's disease, multiple system atrophy, and progressive supranuclear palsy. Neurol. Sci. 24, 149–150. http://dx.doi.org/10.1007/s10072-003-0103-5.

Armstrong, M.J., Litvan, I., Lang, A.E., Bak, T.H., Bhatia, K.P., Borroni, B., Boxer, A.L., Dickson, D.W., Grossman, M., Hallett, M., Josephs, K.A., Kertesz, A., Lee, S.E., Miller, B.L., Reich, S.G., Riley, D.E., Tolosa, E., Tröster, A.I., Vidailhet, M., Weiner, W.J., 2013. Criteria for the diagnosis of corticobasal degeneration. Neurology 80, 496–503. http://dx.doi.org/10.1212/WNL.0b013e31827f0fd1.

Badoud, S., Nicastro, N., Garibotto, V., Burkhard, P.R., Haller, S, 2016. Distinct spatiotemporal patterns for disease duration and stage in Parkinson's disease. Eur. J. Nucl. Med. Mol. Imaging 43 (3), 509–516. http://dx.doi.org/10.1007/s00259-015-3176-5.

Booij, J., Andringa, G., Rijks, L.J., Vermeulen, R.J., de Bruin, K., Boer, G.J., Janssen, A.G., van Royen, E.A., 1997a. [^{123}I]FP-CIT binds to the dopamine transporter as assessed by biodistribution studies in rats and SPECT studies in MPTP-lesioned monkeys. Synapse 27, 183–190. http://dx.doi.org/10.1002/(SICI)1098-2396(199711)27:3<183::AID-SYN4>3.0.CO;2-9.

Booij, J., Tissingh, G., Winogrodzka, A., Boer, G.J., Stoof, J.C., Wolters, E.C., van Royen, E.A., 1997b. Practical benefit of [^{123}I]FP-CIT SPET in the demonstration of the dopaminergic deficit in Parkinson's disease. Eur. J. Nucl. Med. 24, 68–71. http://dx.doi.org/10.1007/BF01728311.

Braak, H., Braak, E., 2000. Pathoanatomy of Parkinson's disease. J. Neurol. 247 (Suppl. 2), II3–I10.

Brooks, D.J., 2010. Imaging dopamine transporters in Parkinson's disease. Biomark. Med 4, 651–660. http://dx.doi.org/10.2217/bmm.10.86.

Brooks, D.J., 2012. Can imaging separate multiple system atrophy from Parkinson's disease? Mov. Disord. 27, 3–5. http://dx.doi.org/10.1002/mds.24046.

Brooks, D.J., IBANEZ, V., Sawle, G.V., Quinn, N., Lees, A.J., MATHIAS, C.J., BANNISTER, R., Marsden, C.D., Frackowiak, R., 1990. Differing patterns of striatal F-18 dopa uptake in Parkinsons-disease, multiple system atrophy, and progressive supranuclear palsy. Ann. Neurol. 28, 547–555. http://dx.doi.org/10.1002/ana.410280412.

Brücke, P.D.T., Asenbaum, S., Pirker, W., Djamshidian, S., Wenger, S., Wöber, C., Müller, C., Podreka, I., 1997. Measurement of the dopaminergic degeneration in Parkinson's disease with [^{123}I]β-CIT and SPECT. Advances in Research on Neurodegeneration, Journal of Neural Transmission. Supplementa. Springer Vienna, Vienna, pp. 9–24 http://dx.doi.org/10.1007/978-3-7091-6842-4_2.

Cummings, J.L., Henchcliffe, C., Schaier, S., Simuni, T., Waxman, A., Kemp, P., 2011. The role of dopaminergic imaging in patients with symptoms of dopaminergic system neurodegeneration. Brain 134, 3146–3166. http://dx.doi.org/10.1093/brain/awr177.

Fazekas, F., Chawluk, J.B., Alavi, A., Hurtig, H.I., Zimmerman, R.A., 1987. MR signal abnormalities at 1.5 T in Alzheimer's dementia and normal aging. AJ. Am. J. Roentgenol. 149, 351–356. http://dx.doi.org/10.2214/ajr.149.2.351.

Friston, K., 2012. Ten ironic rules for non-statistical reviewers. NeuroImage 61, 1300–1310. http://dx.doi.org/10.1016/j.neuroimage.2012.04.018.

Gaig, C., Martí, M.J., Tolosa, E., Valldeoriola, F., Paredes, P., Lomeña, F.J., Nakamae, F., 2006. ^{123}I-Ioflupane SPECT in the diagnosis of suspected psychogenic Parkinsonism. Mov. Disord. 21, 1994–1998. http://dx.doi.org/10.1002/mds.21062.

García-Gómez, F.J., García-Solís, D., Luis-Simón, F.J., Marín-Oyaga, V.A., Carrillo, F., Mir, P., Vázquez-Albertino, R.J., 2013. Elaboration of the SPM template for the standardization of SPECT images with ^{123}I-Ioflupane. Revista Española de Medicina Nuclear e Imagen Molecular (English Edition). 32, pp. 350–356. http://dx.doi.org/10.1016/j.remnie.2013.09.003.

Garibotto, V., Montandon, M.L., Viaud, C.T., Allaoua, M., Assal, F., Burkhard, P.R., Ratib, O., Zaidi, H., 2013. Regions of interest-based discriminant analysis of DaTSCAN SPECT and FDG-PET for the classification of dementia. Clin. Nucl. Med. 38, e112–e117. http://dx.doi.org/10.1097/RLU.0b013e318279b991.

Gilman, S., Wenning, G.K., Low, P.A., Brooks, D.J., MATHIAS, C.J., Trojanowski, J.Q., Wood, N.W., Colosimo, C., Dürr, A., Fowler, C.J., Kaufmann, H., Klockgether, T., Lees, A., Poewe, W., Quinn, N., Revesz, T., Robertson, D., Sandroni, P., Seppi, K., Vidailhet, M., 2008. Second consensus statement on the diagnosis of multiple system atrophy. Presented at the Neurology. Lippincott Williams & Wilkins, pp. 670–676 http://dx.doi.org/10.1212/01.wnl.0000324625.00404.15.

Haller, S., Badoud, S., Nguyen, D., Garibotto, V., Lovblad, K.O., Burkhard, P.R., 2012. Individual detection of patients with Parkinson disease using support vector machine analysis of diffusion tensor imaging data: initial results. AJNR Am. J. Neuroradiol. http://dx.doi.org/10.3174/ajnr.A3126.

Haller, S., Badoud, S., Nguyen, D., Barnaure, I., Montandon, M.-L., Lovblad, K.O., Burkhard, P.R., 2013. Differentiation between Parkinson disease and other forms of Parkinsonism using support vector machine analysis of susceptibility-weighted imaging (SWI): initial results. Eur. Radiol. 23, 12–19. http://dx.doi.org/10.1007/s00330-012-2579-y.

Hughes, A.J., Daniel, S.E., Ben-Shlomo, Y., Lees, A.J., 2002. The accuracy of diagnosis of parkinsonian syndromes in a specialist movement disorder service. Brain 125, 861–870.

Italian Neurological Society, 2003. The diagnosis of Parkinson's disease. Italian Society of Clinical Neurophysiology, Guidelines for the Treatment of Parkinson's Disease 2002. Presented at the Neurological sciences: official journal of the Italian Neurological Society and of the Italian Society of Clinical Neurophysiology, pp. S157–S164 http://dx.doi.org/10.1001/archinte.144.11.2146.

Joutsa, J., Johansson, J., Seppänen, M., Noponen, T., Kaasinen, V., 2015. Dorsal-to-ventral shift in midbrain dopaminergic projections and increased thalamic/raphe serotonergic function in early Parkinson disease. J. Nucl. Med. 56, 1036–1041. http://dx.doi.org/10.2967/jnumed.115.153734.

Kaasinen, V., Gardberg, M., Röyttä, M., Seppänen, M., Päivärinta, M., 2013. Normal dopamine transporter SPECT in neuropathologically confirmed corticobasal degeneration. J. Neurol. 260, 1410–1411. http://dx.doi.org/10.1007/s00415-013-6886-2.

Kägi, G., Bhatia, K.P., Tolosa, E., 2010. The role of DAT-SPECT in movement disorders. J. Neurol. Neurosurg. Psychiatry 81, 5–12. http://dx.doi.org/10.1136/jnnp.2008.157370.

Klaffke, S., Kuhn, A.A., Plotkin, M., Amthauer, H., Harnack, D., Felix, R., Kupsch, A., 2006. Dopamine transporters, D2 receptors, and glucose metabolism in corticobasal degeneration. Mov. Disord. 21, 1724–1727. http://dx.doi.org/10.1002/mds.21004.

Koch, W., Unterrainer, M., Xiong, G., Bartenstein, P., Diemling, M., Varrone, A., Dickson, J.C., Tossici-Bolt, L., Sera, T., Asenbaum, S., Booij, J., Kapucu, O.L., Kluge, A., Ziebell, M., Darcourt, J., Nobili, F., Pagani, M., Hesse, S., Vander Borght, T., Van Laere, K., Tatsch, K., la Fougère, C., 2014. Extrastriatal binding of [^{123}I]FP-CIT in the thalamus and pons: gender and age dependencies assessed in a European multicentre database of healthy controls. Eur. J. Nucl. Med. Mol. Imaging 41, 1938–1946. http://dx.doi.org/10.1007/s00259-014-2785-8.

Leroy, C., Karila, L., Martinot, J.L., Lukasiewicz, M., Duchesnay, E., Comtat, C., Dollé, F., Benyamina, A., Artiges, E., Ribeiro, M.J., Reynaud, M., Trichard, C., 2012. Striatal and extrastriatal dopamine transporter in cannabis and tobacco addiction: a high-resolution PET study. Addict. Biol. 17, 981–990. http://dx.doi.org/10.1111/j.1369-1600.2011.00356.x.

Litvan, I., Agid, Y., Jankovic, J., Goetz, C., Brandel, J.P., Lai, E.C., Wenning, G., D'Olhaberriague, L., Verny, M., Chaudhuri, K.R., McKee, A., Jellinger, K., Bartko, J.J., Mangone, C.A., Pearce, R.K., 1996. Accuracy of clinical criteria for the diagnosis of progressive supranuclear palsy (Steele-Richardson-Olszewski syndrome). Neurology 46, 922–930.

Marek, K., Seibyl, J., Holloway, R., Kieburtz, K., Oakes, D., Lang, A., Yim, J., Dey, H., Cellar, J., Fussell, B., Broshjeit, S., Early, M., Smith, E.O., Sudarsky, L., Johnson, K.A., Corwin, C., Johnson, D., Lajoie, S., Reich, S.G., Frost, J.J., Goldberg, P., Flesher, J.E., Feigin, A., Mazurkiewicz, J., Castronuovo, J., Joseph, F., DiRocco, A., Olanow, C.W., Machac, J., Cotei, D., Webner, P., Rudolph, A., Day, D., Casaceli, C., Freimuth, A., Orme, C., Hodgeman, K., Eberly, S., Henry, E., Morgan, G., Haley, J.B., Grp, P.S., 2000. A multicenter assessment of dopamine transporter imaging with DOPASCAN/SPECT in parkinsonism. Neurology 55, 1540–1547.

Nicastro, N., Garibotto, V., Poncet, A., Badoud, S., Burkhard, P.R., 2016. Establishing on-site reference values for ^{123}I-FP-CIT SPECT (DaTSCAN®) using a cohort of individuals with non-degenerative conditions. Mol. Imaging Biol. 18 (2), 302–312. http://dx.doi.org/10.1007/s11307-015-0889-6.

Nocker, M., Seppi, K., Donnemiller, E., Virgolini, I., Wenning, G.K., Poewe, W., Scherfler, C., 2012. Progression of dopamine transporter decline in patients with the Parkinson variant of multiple system atrophy: a voxel-based analysis of [^{123}I]β-CIT SPECT. Eur. J. Nucl. Med. Mol. Imaging 39, 1012–1020. http://dx.doi.org/10.1007/s00259-012-2100-5.

Palumbo, B., Fravolini, M.L., Buresta, T., Pompili, F., Forini, N., Nigro, P., Calabresi, P., Tambasco, N., 2014. Diagnostic accuracy of Parkinson disease by support vector machine (SVM) analysis of ^{123}I-FP-CIT brain SPECT data. Medicine 93, e228. http://dx.doi.org/10.1097/MD.0000000000000228.

Pirker, W., Asenbaum, S., Bencsits, G., Prayer, D., Gerschlager, W., Deecke, L., Brücke, T., 2000a. [^{123}I]beta-CIT SPECT in multiple system atrophy, progressive supranuclear palsy, and corticobasal degeneration. Mov. Disord. 15, 1158–1167.

Pirker, W., Asenbaum, S., Bencsits, G., Prayer, D., Gerschlager, W., Deecke, L., Brücke, T., 2000b. [^{123}I]β-CIT spect in multiple system atrophy, progressive supranuclear palsy, and corticobasal degeneration. Mov. Disord. 15, 1158–1167. http://dx.doi.org/10.1002/1531-8257(200011)15:6<1158::AID-MDS1015>3.0.CO;2-0.

Rokach, L., 2010. Pattern Classification Using Ensemble Methods. Series in Machine Perception and Artificial Intelligence. Vol. 75. World Scientific Publishing Co. Pte. Ltd.

Scherfler, C., Seppi, K., Donnemiller, E., Goebel, G., Brenneis, C., Virgolini, I., Wenning, G.K., Poewe, W., 2005. Voxel-wise analysis of [^{123}I]beta-CIT SPECT differentiates the Parkinson variant of multiple system atrophy from idiopathic Parkinson's disease. Brain 128, 1605–1612. http://dx.doi.org/10.1093/brain/awh485.

Segovia, F., Górriz, J.M., Ramirez, J., Alvarez, I., Jimenez-Hoyuela, J.M., Ortega, S.J., 2012. Improved Parkinsonism diagnosis using a partial least squares based approach. Med. Phys. 39, 4395–4403. http://dx.doi.org/10.1118/1.4730289.

Seibyl, J., Jennings, D., Grachev, I., Coffey, C., Marek, K., 2013. 123-I Ioflupane SPECT measures of Parkinson disease progression in the Parkinson Progression Marker Initiative (PPMI) trial. J. Nucl. Med.

Seppi, K., Scherfler, C., Donnemiller, E., Virgolini, I., Schocke, M.F.H., Goebel, G., Mair, K.J., Boesch, S., Brenneis, C., Wenning, G.K., Poewe, W., 2006. Topography of dopamine transporter availability in progressive supranuclear palsy: a voxelwise [^{123}I]β-CIT SPECT analysis. Arch. Neurol. 63, 1154–1160. http://dx.doi.org/10.1001/archneur.63.8.1154.

Sixel-Döring, F., Liepe, K., Mollenhauer, B., Trautmann, E., Trenkwalder, C., 2011. The role of ^{123}I-FP-CIT-SPECT in the differential diagnosis of Parkinson and tremor syndromes: a critical assessment of 125 cases. J. Neurol. 258, 2147–2154. http://dx.doi.org/10.1007/s00415-011-6076-z.

Smith, S.M., Nichols, T.E., 2009. Threshold-free cluster enhancement: addressing problems of smoothing, threshold dependence and localisation in cluster inference. NeuroImage 44, 83–98. http://dx.doi.org/10.1016/j.neuroimage.2008.03.061.

Tahir, N.M., Manap, H.H., 2012. Parkinson disease gait classification based on machine learning approach. J. Appl. Sci.

Varrone, A., Marek, K.L., Jennings, D., Innis, R.B., Seibyl, J.P., 2001. [^{123}I]β-CIT SPECT imaging demonstrates reduced density of striatal dopamine transporters in Parkinson's disease and multiple system atrophy. Mov. Disord. 16, 1023–1032. http://dx.doi.org/10.1002/mds.1256.